ChemPubSoc Europe

DOI: 10.1002/chem.201xxxxxx

CHEMISTRY
A European Journal
Full Paper

Pharmaceuticals

Insights into the Crystallisation Process from Anhydrous, Hydrated and Solvated Crystal Forms of Diatrizoic Acid

Katharina Fucke,*[a] Garry J. McIntyre,[b,c] Marie-Hélène Lemée-Cailleau,[d] Clive Wilkinson,[b,d] Alison J. Edwards,[c] Judith A. K. Howard,[b] Jonathan W. Steed*[b]

Abstract: Diatrizoic acid (DTA), a clinically used X-ray contrast agent, crystallises in two hydrated, three anhydrous and nine solvated solid forms, all of which have been characterised by X-ray crystallography. Single crystal neutron structures of DTA dihydrate and monosodium DTA tetrahydrate have been determined. All of the solid state structures have been analysed using partial atomic charges and hardness algorithm (PACHA) calculations. Even though in general all DTA crystal forms reveal similar intermolecular interactions, the overall crystal packing differs considerably from form to form. The water of the dihydrate is encapsulated between a pair of host molecules, which calculations reveal to be an extraordinarily stable motif. DTA presents functionalities that enable hydrogen and halogen bonding, and whilst an extended hydrogen bonding network is realised in all crystal forms, the halogen bonding is not present in the hydrated crystal forms. This is due to the formation of a hydrogen-bonding network based on individual enclosed water squares, which is not amenable to the concomitant formation of halogen bonds. The main interaction in the solvates involves the carboxylic acid, which corroborates the hypothesis that this strong interaction is the last one to be broken during the crystal desolvation and nucleation process.

Introduction

Pharmaceutically relevant small organic molecules tend to exist in more than one crystal form.[1] These materials can represent different crystalline arrangements of the compound itself leading to polymorphs, which differ either by the conformation of the molecule, by the overall packing, or by a combination of both.[2] In addition, solvent molecules from the crystallisation process can be included into the crystal lattice, leading to hydrates in the case of incorporated water and solvates for any other solvent.[3] Both hydrates and solvates are a special case of co-crystal formation.[4] Different crystal forms can exhibit quite varied physico-chemical characteristics, ranging from physical and chemical stability to solubility and rate of dissolution. The latter two are important especially for pharmaceutical compounds, as the drug has to dissolve in aqueous body fluids in order to be taken up into cells and tissues to reach the target biological receptors. Thus, low solubility directly affects the bio-availability and must be addressed during drug formulation.

Polymorphism in pharmaceutical materials is widely studied,[5] and normally every newly developed drug compound is subjected to extensive crystal form screening[5c] in order to discover as many of the experimentally accessible polymorphs and solvates, particularly hydrates, as possible.[6]

However, this approach is money- and time-consuming and it does not guarantee the isolation of all possible stable crystal forms, as cases such as that of Ritonavir show.[7] Thus, a more fundamental understanding of the factors leading to different

[a] *Dr. K. Fucke,*
School of Medicine, Pharmacy and Health, Durham University
University Boulevard, Stockton-on-Tees, TS17 6BH, United Kingdom
Fax: +44 191 +
E-mail: Katharina.Fucke@durham.ac.uk

[b] *Dr. G.J. McIntyre, Dr. C. Wilkinson, Prof. J.A.K. Howard, Prof. J.W. Steed*
Department of Chemistry, Durham University
South Road, Durham, DH 13LE, United Kingdom
Fax: +44 191 384 4737
E-mail: Jon.Steed@durham.ac.uk

[c] *Dr. A.J. Edwards, Dr. G.J. McIntyre*
The Bragg Institute
Australian Nuclear Science and Technology Organisation, Locked Bag 2001, Kirrawee DC NSW 2234, Australia

[d] *Dr M.-H. Lemée-Cailleau, Dr. C. Wilkinson*
Institut Laue-Langevin
6 Rue Horowitz, 38042 Grenoble Cedex, France

((If supporting information is submitted, please include the following line:))
Supporting information for this article is available on the WWW under http://www.chemeurj.org/ or from the author.

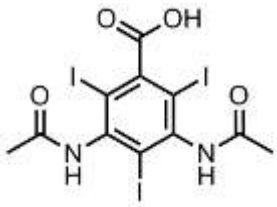

Scheme 1. Molecular structure of diatrizoic acid.

polymorphic and solvated crystal forms is an ongoing key objective.[5a, 8]

On the molecular level, drug compounds generally contain a range of functional groups, which allow them to interact with the target protein, receptor or enzyme, to show a pharmacological effect. As a result, pharmaceuticals are relatively complicated small molecules and, to date little is known about the factors influencing their polymorphism and hydrate/solvate formation. In particular the interplay of the mutual interactions of the functional groups on the drug molecules themselves and their interactions with solvent molecules during crystallisation from solution or the melt is rarely investigated.[9] Extensive information of this type however, as has been obtained for the widely studied carbamazepine,[10] will lead to an understanding of why and how different solid forms can be crystallised, and how certain forms can be avoided.

Two directional intermolecular interactions play a key role during crystallisation and in the crystalline state, namely hydrogen bonding and halogen bonding.[11] Hydrogen bonding has been found to stabilise crystal structures and to play a major role in how a molecule will arrange in the solid state.[12] Due to its accessibility and relative low cost, most studies into the characteristics of hydrogen bonds are based on X-ray single-crystal diffraction; however, accurate location of hydrogen atoms requires the use of single crystal neutron diffraction.[13] Accurate neutron structural data are thus of key importance in determining the experimental charge density.[14] They are also used to investigate the energetic contribution of the hydrogen bond to the overall crystal lattice energy by using the Partial Atomic Charges and Hardness Algorithm (PACHA).[15]

In addition to hydrogen bonding, halogen bonds are increasingly recognised as a key directional interaction in molecular crystal structures.[16] Even though these interactions are generally considerably weaker than hydrogen bonds, they have been shown in recent years to comprise a significant stabilising interaction,[17] with interesting work reported on the competition of hydrogen *versus* halogen bonding in molecular crystals.[18] Halogen bonding has been shown to persist in solution-state anion receptors[19] and can drive gelation behaviour.[17a]

In this study, we seek to understand the interplay of hydrogen and halogen bonding and their influence on the crystal forms of an X-ray contrast molecule, diatrizoic acid (DTA, Scheme 1), which is pharmaceutically relevant and listed in the European[20] and United States Pharmacopoeias[21] as the dihydrated form. Specifically monographed crystal forms are generally prevalent and stable enough for manufacture, and since DTA is poorly water soluble, the formation of a hydrate indicates severe problems for pharmaceutical manufacturing, because hydrates show thermodynamically the lowest solubility in water of all crystal forms of a specific compound.[22] This problem has

Figure 1. Photo micrographs of the diatrizoic acid hydrated crystal forms: a) DTA dihydrate, b) DTS tetrahydrate initial blades and c) DTS tetrahydrate final blocks.

been circumvented by the formulation of DTA as a pharmaceutically acceptable salt form, either as sodium (diatrizoate sodium, DTS), meglumine or L-lysinium salt or a mixture thereof, as a commercially available *intra-venous* preparation. While the sodium salt also crystallises in a highly hydrated form,[23] the solubility of the charged species in water is considerably higher than that of the free acid. Another new application of the contrast molecule is its immobilisation on the surface of gold nanoparticles for *IV* administration as contrast for enhanced computed tomography.[24]

The DTA molecule has two amide NH groups and one carboxylic acid OH functionality as hydrogen-bond donors, as well as two amide and one carboxylic acid carbonyl groups as hydrogen-bond acceptors. This balanced ratio of donors and acceptors suggests that the substance might be expected to crystallise in extensive hydrogen-bonded networks. The three iodo substituents present the additional possibility of halogen-bonding interactions, particularly with halogen-bond accepting solvents. Folen *et al*. have reported the dihydrate form of DTA as well as an additional anhydrous modification, which in this study will be referred to as form I.[25] We have previously reported three dimethylsulfoxide solvates of DTA giving insight into the desolvation of the compound during crystallisation,[26] as well as the crystal structure of the disodium salt.[27] We now report a wide-ranging study on DTA polymorphism and solvate formation in order to elucidate the factors governing the interplay of hydrogen bonding and halogen bonding in particular and shed light onto the desolvation and crystallisation process in this versatile system.

Results

The crystal forms

Diatrizoic acid was found to exist in two hydrated forms: the known dihydrate[25] and a new form which contains one water molecule per four host molecules (a tetarto hydrate). In addition, three anhydrous modifications, named forms I, II and III in the order of their discovery, were obtained. Form I has been previously reported by Folen and co-workers[25] and crystallises only from the melt, while forms II and III can only be obtained by thermal dehydration of the dihydrate. In addition, solvates containing dimethyl formamide, methanol, tetrahydrofuran, dioxane/water and dimethyl sulfoxide have been isolated.

DTA dihydrate

DTA is very sparingly soluble in water at room temperature, while the solubility increases significantly upon heating to boiling point. On cooling this solution, prismatic block-shaped crystals of the dihydrate grow within a couple of hours, and their crystal size depends on the cooling rate. Large, high quality crystals (Figure 1a) were obtained by very slow cooling of a saturated aqueous

Table 1. X-ray crystallographic data of the crystal forms.

Parameter	DTA dihydrate	DTS tetrahydrate	DTA form I	DTA tetarto hydrate	DTA DMF disolvate	DTA THF monosolvate	DTA dioxane/water monosolvate	DTA methanol monosolvate
Formula	$C_{11}H_9O_4N_2I_3 \cdot 2\ H_2O$	$C_{11}H_8O_4N_2I_3Na \cdot 4.25\ H_2O$	$C_{11}H_9O_4N_2I_3$	$C_{11}H_9O_4N_2I_3 \cdot 0.25\ H_2O$	$C_{11}H_9I_3N_2O_4 \cdot 2\ (C_3H_7NO)$	$C_{11}H_9I_3N_2O_4 \cdot C_4H_8O$	$C_{11}H_9I_3N_2O_4 \cdot H_2O \cdot C_4H_8O_2$	$C_{11}H_9I_3N_2O_4 \cdot CH_4O$
M_r	649.93	1421.88	613.90	622.91	760.11	686.03	720.04	645.96
Crystal system	triclinic	triclinic	monoclinic	monoclinic	orthorhombic	monoclinic	monoclinic	triclinic
Space group	*P*-1	*P*-1	*C2/c*	*C2/c*	*Pbca*	$P2_1/n$	$P2_1/n$	*P*-1
T (K)	120	120	120	120	120	120	150	120
a (Å)	7.8264(6)	11.754(2)	20.646(4)	20.70(2)	21.321(3)	8.893(1)	11.940(4)	9.4497(1)
b (Å)	9.4397(8)	13.091(3)	9.353(2)	9.407(8)	9.277(1)	18.818(2)	11.878(4)	13.9552(2)
c (Å)	13.302(1)	15.129(4)	18.688(3)	18.68(2)	25.724(1)	12.767(1)	15.642(5)	14.6126(2)
α (°)	89.673(2)	73.62(2)	90	90	90	90	90	85.214(1)
β (°)	75.570(2)	84.56(2)	117.020(5)	116.440(8)	90	90.188	100.925(3)	87.695(1)
γ (°)	71.091(2)	63.50(1)	90	90	90	90	90	72.367(1)
V (Å3)	897.4(1)	2024.1(8)	3215(1)	3257(5)	5088(1)	2136.5(4)	2178(1)	1829.83(4)
Z	2	2	8	8	8	4	4	4
R_1 (%)	2.16	2.12	4.59	7.40	2.51	4.40	4.42	2.46

solution containing minor amounts of ethanol as solubiliser from boiling point to room temperature.

DTA dihydrate crystallises in the triclinic space group $P\bar{1}$ with one formula unit in the asymmetric unit (Z' = 1, Table 1, supplementary information Table S1). The host molecule adopts a conformation in which both amide substituents as well as the carboxylic acid group are rotated out of the aromatic ring plane, with the oxygen atoms of the amide groups and the hydroxyl function of the acid group being on the same side of the ring in a *syn*-conformation. Four water molecules are sandwiched between pairs of DTA hosts in a hydrogen bonded square (Figure 2a). Two of these donate hydrogen bonds to the carbonyl groups of DTA, while the other two accept one hydrogen bond from the acid group of the host forming a hydrogen-bonded capsule, resembling the water squares encapsulated in tetrapodal urea complexes characterised by neutron diffraction.[28]

The stacking of this basic DTA-water-capsule into the 3D crystal network is stabilised through two different hydrogen bonds. Firstly, the capsules stack along (0 0 1) through hydrogen bonding from N1 of an amido group to the non-protonated oxygen atom O2 of the carboxylic acid group of the next capsule (Figure 2b). The second stacking motif involves hydrogen bonding from N2 of the second amido group to O3 of the amido group of an adjacent capsule resulting in stacks along the crystallographic *a*-axis.

This crystal packing results in the formation of layers which are strongly hydrogen bonded. Interestingly, in the direction of the crystallographic *b*-axis, the packing of the layers is only stabilised through weaker C-H···O interactions, and thus the association between layers cannot be as strong as the interactions within the layers.

A single-crystal neutron-diffraction structure determination of DTA dihydrate was undertaken at 120 K using the Laue diffractometer KOALA at the Bragg Institute (Lucas Heights, Australia). Due to the low symmetry of this crystal structure (triclinic, $P\bar{1}$) the Laue diffraction patterns measured for a single orientation of the crystal on the φ axis gave only a restricted amount of data. However, the structural model could be refined to give a stable solution without restraints and all hydrogen atoms could be identified reliably from the Fourier difference maps (Figure 2a).

The hydrogen atom positions in the neutron structure are similar with the positions calculated for the X-ray structure, but with significant differences in the bond lengths. As expected, the terminal CH_3 groups of the host molecule show rather large atomic anisotropic displacement parameters (ADPs) for the hydrogen positions indicating rotational mobility in these groups, which could not be modelled as static disorder and is most likely of dynamic origin. The C-H bonds vary between 0.99(6) and 1.07(5) Å and thus these values are close to the geometrically constrained calculated C-H bonds of the X-ray model (0.98 Å).

As all of the remaining hydrogen atoms in the X-ray crystal structure were located from the difference Fourier maps and refined freely, the atomic positions are a compromise between experimental electron density and electrostatic energy optimisation employed in the algorithm of olex.refine.[29] For this reason, the directionality of the X-H bond fits well with that found in the neutron structure, whilst the bond distances vary to up to 0.3 Å (Table S2). This fact has a major influence on the hydrogen bonding energies and strengths of these interactions in the subsequent calculations.

The atomic coordinates derived from the neutron structure determination were used for semi-empirical lattice energy calculations using PACHA.[15c] Even though the results of these calculations have to be interpreted with caution due to the algorithm treating the atoms as point charges and calculating only dipolar interactions excluding higher order effects, the extracted energies give a good approximation of the ranking of interaction strength, and cope well with many-atom structures at modest computational cost. The results of the PACHA calculations are listed in Table 2. Starting from the host-host interactions of the DTA dihydrate, both homomeric hydrogen bonds donated by amido N-H moieties to either an adjacent amido oxygen atom or the carboxylic acid group show energies in the range of medium–to-strong hydrogen bonds.[12b] Interestingly, the hydrogen bond with the carboxylic acid moiety as acceptor is only slightly stronger than the one having an amide carbonyl group as acceptor. All hydrogen bonds involving the water molecules are considerably stronger than the homomeric host to host interactions. The hydrogen bonds between O1W and O2W in the water square have a stabilising energy of almost double the value compared to the homomeric interactions.

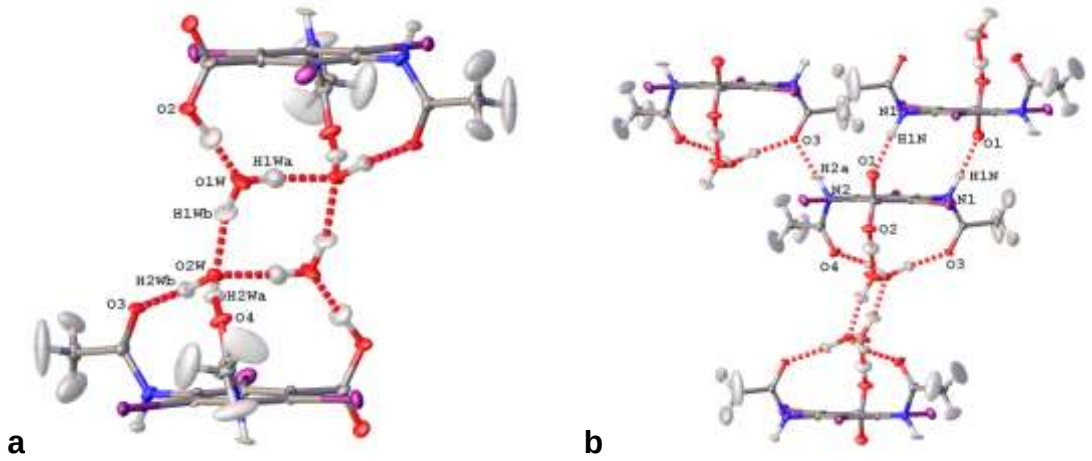

Figure 2 (a) Discrete water square found "encapsulated" between two DTA molecules in DTA dihydrate and (b) stacking motifs found in the structure of DTA dihydrate as derived from the single-crystal neutron structure. Ellipsoids are drawn at 30 % probability.

Table 2. Geometric and energetic data for DTA dihydrate.

Interaction[a]	D···A distance [Å]	H···A distance [Å]	D-H···A angle [°]	Energy [kJ mol^{-1}][b]
O2-H2···O1W	2.49(2)	1.45(3)[a]	177(2)	-56.4
N1-H1···O2	2.80(2)	1.81(3)	175(1)	-16.6
N2-H2a···O3	2.82(1)	1.82(2)[a]	172(1)	-15.1
O1W-H1Wa···O2W	2.68(3)	1.72(3)[a]	165(1)	-28.5
O1W-H1Wb···O2W	2.72(2)	1.77(3)[a]	174(2)	-28.5
O2W-H2Wa···O4	2.67(2)	1.73(2)[a]	163(2)	-34.0

[a] Hydrogen···acceptor distance derived from the neutron single crystal data.
[b] Interaction energies as calculated by the PACHA algorithm.

The heteromeric hydrogen bonds between the incorporated water molecules O2W and the host carbonyl oxygen atoms are even stronger. The strongest interaction, however, is the hydrogen bond donated from the carboxylic acid OH group of the host to the oxygen atom O1W of the water molecule, which is consistent with our previous work on DMSO solvates of DTA,[26] in which the hydrogen bonds donated from the acid of DTA are the strongest and hence are expected to be broken last during desolvation during the crystal nucleation process. It is, however, surprising how short this interaction is, with only 1.45 Å distance between the hydrogen atom and the acceptor oxygen atom. It is possible that this hydrogen atom can move between the donor and the acceptor oxygen at elevated temperatures, as has been shown for a dimethylurea co-crystal,[30] but since the neutron structure has been determined at 120 K, the hydrogen atom is frozen in a more localised position. Because of the considerably stronger interactions between the host and the water molecules compared to the inter-host homomeric interactions, DTA dihydrate is in some sense the opposite to theophylline monohydrate,[15a] in which the homomeric interactions are considerably stronger than those between the host and the water molecules. As a result theophylline monohydrate is relatively unstable and readily dehydrates leaving the overall structural network intact.[15a] It is also likely that since the water square embedded within the DTA dimeric capsule represents such a robust supramolecular motif, that these capsular structures may exist in solution before any stable crystal nuclei form.

Thermo-microscopic investigations showed that the dihydrate crystals remain unchanged between room temperature and 120 °C. Upon further heating, the crystals start to move and jump whilst undergoing pseudomorphosis, indicating radical changes to the crystal structure.[31] A preparation of the dihydrate in paraffin oil shows bubble formation accompanying the pseudomorphosis verifying the release of water, which is complete at about 135 °C. Dehydration at such high temperatures is unusual for organic hydrates without cation coordination of the incorporated water and demonstrates the extraordinary stability of this crystal form. Upon further heating sublimation into fine needles can be observed above 300 °C, while above 320 °C the sample melts and decomposes concomitantly.

The analysis of the thermogravimetry (TG) (Figure 3) confirms the high stability of DTA dihydrate. The thermogram shows no weight loss of the sample up to 80 °C, while a following single step of 5.68% weight loss represents the release of the crystal water (calculated value for a dihydrate is 5.54%). The dehydration temperature detected in the TG is lower than that observed by thermo-microscopy which is due to the dynamic dry helium flow around the sample. The dehydrated sample is stable to 290 °C, above which a second weight loss indicates decomposition during which volatile decomposition products are released.

The observed thermal behaviour of DTA dihydrate is reflected in its differential scanning calorimetry (DSC) trace (Figure 3). The thermogram shows a dehydration endotherm in the temperature range from 80 to 150 °C, which coincides with the mass loss found by TG. The crystal form present after this dehydration event was verified by FTIR measurements to be a new anhydrous form, Form II, as compared to the spectra of the dihydrate and the previously published anhydrous Form I. Upon further heating, Form II transforms in an exothermic event into anhydrous Form III, a second new crystal form. Exothermic transitions generally imply a monotropic relationship between the two crystal forms.[32]

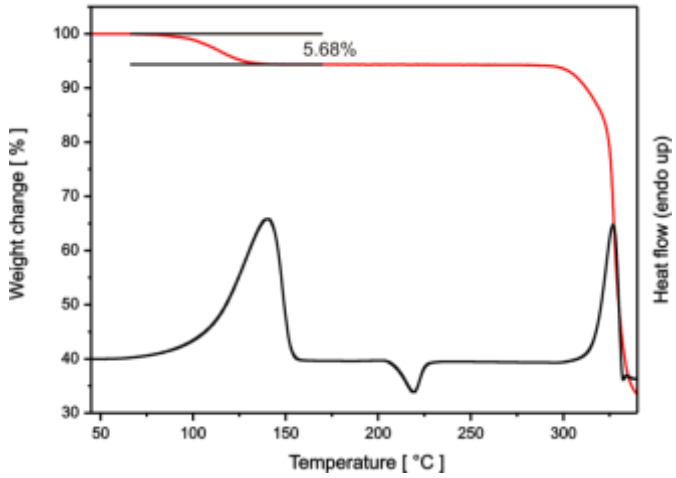

Figure 3. Thermogravimetric (upper curve) and differential scanning calorimetric (lower curve) thermograms of DTA dihydrate, both recorded at 10 °C min^{-1}.

With the thermal data listed in Table 3, a semi-schematic energy/temperature diagram was constructed (Figure 4).[32-33] It is clearly visible that the *G*-isobars of the two polymorphs run in parallel over the whole temperature range and do not intersect. Thus, these two crystal forms are monotropically related to each other, and Form III is the thermodynamically stable polymorph at all temperatures. Unfortunately, it was not possible to obtain single crystals suitable for structure determination of either of these two crystal forms, however their powder X-ray diffraction (PXRD) patterns and FTIR spectra are presented in the supporting information (ESI Figures S1 and S2). Due to the high absorption of the DTA molecule caused by the three iodine substituents, the PXRD patterns of Forms II and III are very low in intensity. However, clear changes in peak positions can be seen, proving that a phase transition occurred. The same change can be detected by FTIR spectroscopy. The most striking changes are in the OH and NH vibrational region around 3500 cm^{-1}, which changes significantly from the dihydrate to its dehydrated Form II. Surprisingly, Form III has a sharp peak in this region, which points towards a very distinct hydrogen-bonding pattern involving the carboxylic acid or the amido NH groups. This assumption is supported by the changes detected in the carbonyl stretch vibrations at around 1700 cm^{-1}. Another region of changes is between 1700 and 1600 cm^{-1}, in which the aromatic ring vibrations are located. For phase identification, even though the exact nature of the vibrations is hard to establish, the fingerprint region offers unique patterns for each of the three crystal forms.

Table 3. Thermal data of the solid state transitions of the anhydrous crystal forms of DTA.

	Transition temperature (onset) [°C]	Heat of transition [kJ mol^{-1}]	Melting point (onset) [°C]	Heat of fusion [kJ mol^{-1}]
Form II	210.8±0.4	-7.3±0.3		
Form III			306.7±2.3	31.6±1.7

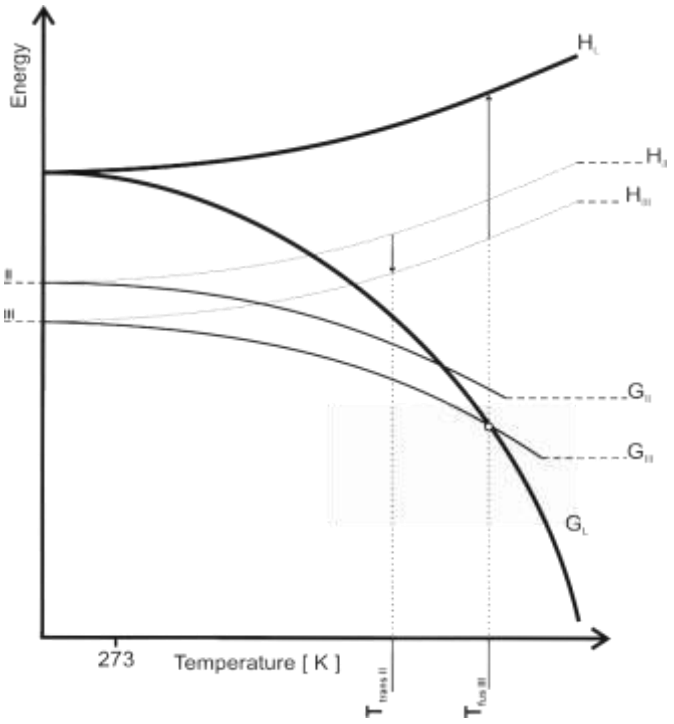

Figure 4. Semi-schematic energy/temperature diagram of the DTA anhydrous forms II and III.

DTA tetartohydrate

In addition to the DTA dihydrate, a second hydrated structure of DTA was crystallised from 1-propanol (Table 1). The single-crystal X-ray data can be successfully modelled as containing 0.25 molecules of water making this crystal form a tetartohydrate. The crystal structure contains the host molecule in a different conformation to the dihydrate, in which the two amide carbonyl oxygen atoms lie on opposite sides of the ring. This *trans* conformation causes the assembly of a different hydrogen-bonded network, based on stacks along the crystallographic *b*-axis, consisting of centrosymmetric dimers connected through hydrogen bonds from the amide N2 to the amide carbonyl O3 (Figure 5). The connection of these dimers is also found in the structures of the dihydrate, and involves two hydrogen bonds from the amide N1 to the acid group O2 connecting two of the host molecules in a centrosymmetric fashion. The remaining hydrogen-bond donor of the tetartohydrate, O1 of the carboxylic acid group, interacts with the remaining hydrogen-bond acceptor O4. This last interaction connects the stacks along the crystallographic *c*-axis. The incorporated water molecule is relatively far away from any potential hydrogen bond donor or acceptor, and hydrogen atom positions could not be located in the Fourier maps. However, electrostatic optimisation of the hydrogen positions suggests long distance interactions between the water molecule and the amido carbonyl oxygen atom O4, which would give a bridging connection between two host stacks along the crystallographic *a*-axis.

Table 4. Geometric and energetic data of DTA tetartohydrate and form I.

Interaction[a]	D···A distance [Å]	D-H···A angle [°]	Energy [kJ mol^{-1}]
Tetartohydrate			
O1···O4	2.51(2)	178[a]	-51.9
N1···O2	2.95(2)	175.7(9)	-28.9
N2···O3	2.82(2)	151.8(9)	-36.2
O1W···O4	3.16(3)	172[a]	-18.5
Form I			
O1···O4	2.55(1)	160(6)	-51.1
N1···O2	2.817(9)	150.1(6)	-31.9
N2···O3	2.921(9)	174.3(8)	-29.5

[a] Angle after electrostatic optimisation of the water hydrogen atom positions.

The X-ray crystal structure of the tetartohydrate was determined using synchrotron radiation. The structural model is not of the highest precision due to lack of observed data caused by the small crystal size, thus the PACHA calculations have to be interpreted cautiously. Again, only the energetic trends will be considered. The DTA dimers are both connected through medium-strength hydrogen bonds (Table 4), while the interaction involving the acid group is considerably stronger. This correlates well with the energies found for the dihydrate and the DMSO solvates. The interactions involving the water molecule are rather weak compared to those found in the dihydrate, which is attributed to the long distance of the interacting atoms. However, this low energy can also explain that a crystal form closely related to the tetartohydrate can be grown from the melt completely water-free. This form (Table S1 and Figure 5) corresponds to the anhydrous crystal form described by Folen and co-workers (Form I).[25] In light of the close correlation of the crystal packing as well as the lack of interaction between the host and the hydrate molecules, it is possible that the tetartohydrate shows non-stoichiometric behaviour.

The interaction energies of the tetartohydrate (Table 4) and the considerable distance of the included water molecule to any interacting functional group of the host molecule indicate that the water molecules act mainly as 'space fillers' and that the interactions involving them are not essential for the stability of the crystal structure.

Since the tetartohydrate and Form I are structurally very closely related, it is difficult to determine with certainty, which crystal form was originally described by Folen *et al*.[25] Even though sufficiently large quantities of the pure modification could not be obtained in order to measure experimental PXRD patterns, the calculated patterns show such similarity such that it would be very difficult to differentiate between the two forms with experimental data from lab-based X-ray diffractometers (Figure S4). In addition, as the only method to produce pure Form I is by melting the DMF solvate in a paraffin oil suspension to reach the peritectic melting point, samples of Form I for IR spectroscopy have large quantities of paraffin oil as impurities, which makes a comparison of the IR spectra impossible. Form I is originally also characterised by TG, but the data is only presented from a starting temperature of 40 °C. Taking into account the possible non-stoichiometric behaviour of the tetartohydrate and the calculated overall mass loss of only 0.7%, the release of the water could be easily missed or misinterpreted as loss of surface attached solvent.

DTS tetrahydrate

The monosodium salt of diatrizoic acid has been previously reported by Tonnessen *et al.*[23] and shows a higher solubility in water than DTA and can be crystallised by precipitation from aqueous solution with anti-solvent, *e.g.* acetone. The initial crystals formed are fine blades (Figure 1b), which over time ripen to blocks (Figure 1c). This proved to be due to Ostwald ripening and not to the existence of different crystal forms and a phase transition, as demonstrated by PXRD. Thermomicroscopy shows that these blocks undergo a very strong pseudomorphosis accompanying dehydration between 75 and 79 °C to the extent that the DTS tetrahydrate crystals not only transform into powder but the particles additionally lose all of their initial macroscopic integrity during this event (Figure 6). Having such a marked pseudomorphosis upon phase transition indicates a radical change in the crystal structure during the thermal event. Surprisingly, the dehydration does not take place at very high temperatures, as would be expected for the strongly coordinating hydrates of organic sodium salts.[34] Upon further heating, melting occurs at 278 °C. This event resembles a gradual amorphisation or glass-transition, in which the crystals lose their birefringence without obvious formation of a liquid phase and there is rapid decay of the morphology of the particles. This behaviour is similar to that of polymers, whilst small molecular crystals generally show a sharp melting event, and it is presumably due to concomitant decomposition. Additionally, bubbles form in the resulting melt, which indicates either decomposition or residual water entrapped in the crystals during the dehydration process being released upon melting.

The DTS tetrahydrate is very unstable compared to DTA dihydrate and the TG trace shows the release of the incorporated water starting even at room temperature (Figure 7). This indicates, that the crystal form can be dehydrated by lowering the relative humidity (RH), while samples of the tetrahydrate can be stored unchanged as dry powder under ambient conditions (~40% RH). TGA analysis shows an initial weight loss step of 6.38%, corresponding to 2.4 moles of water. At about 85 °C this mass loss process is complete and the TG trace indicates that the sample is in equilibrium until a second mass loss of 2.08% (0.75 moles of water) occurs in the range 170 to 210 °C. This second event was not observed by thermomicroscopy, which could be due to the small particle size of the corresponding dehydrated crystal form. A third mass loss is detected above 240 °C representing decomposition of the sample. Compared to the DTA dihydrate, this decomposition takes place about 40 °C lower and indicates the lower thermal stability of the sodium salt. The total mass loss before decomposition adds up to 3.15 moles,

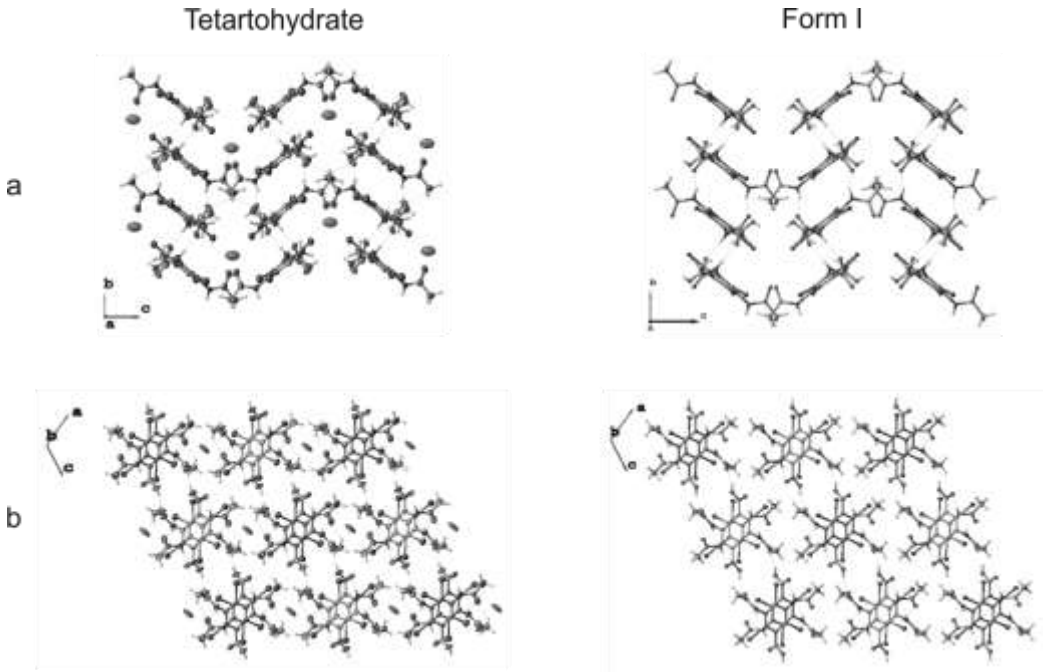

Figure 5 Molecular packing of the DTA tetartohydrate and the anhydrous form I viewed (a) along (1 0 0) and (b) along (0 1 0). For colour version see Figure S3.

Figure 6 Photo micrographs of the dehydration of DTS tetrahydrate upon heating. The first micrograph is taken at 74 °C with the following images taken every 5 seconds at a heating rate of 10 °C min^{-1}.

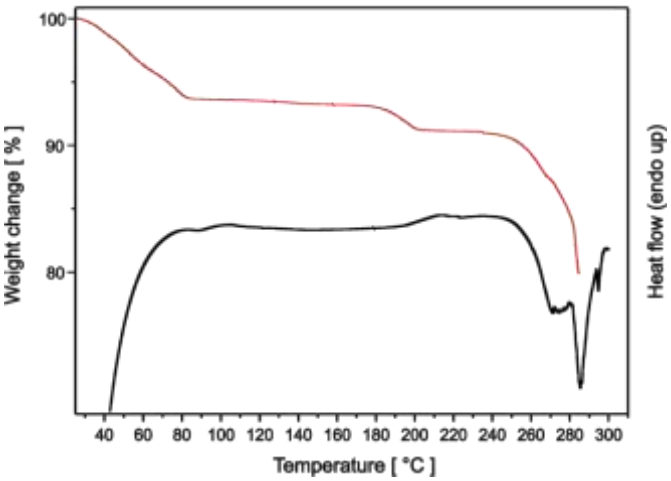

Figure 7. Thermogravimetric (upper curve) and differential scanning calorimetric (lower curve) thermograms of DTS tetrahydrate, both recorded at 10 °C min^{-1}.

considerably lower than the 4 moles anticipated for a tetrahydrate. TG-MS measurements revealed that water is released from the sample during both dehydration steps but also during the decomposition step. This water has to be crystal water rather than decomposition product and would explain the discrepancy between the calculated and the experimental water loss. However, it cannot be excluded that the sample loses crystal water during storage or when the sample is initially put into the dry purge gas of the TG, and it is possible that the lower than expected mass loss is due to a combination of these processes.

The DSC trace of DTS tetrahydrate matches the unstable behaviour observed by TG. Two endothermic events can be detected, the first at approximately 90 °C, which correlates with the first dehydration. The second event starts at 190 °C, matching the second weight loss observed by TG. Above this temperature, a very pronounced exothermic event represents the decomposition of the sample and is in good agreement with the results of the TG experiment.

Block-shaped single crystals of the DTS tetrahydrate turned out to be twinned and represent presumably an aggregation of the initially crystallising blades. However, the single-crystal X-ray structure was redetermined for further use as initial model for the neutron structure refinement. We could confirm the model published earlier by Tonnessen *et al.*[23] with two formula units in the asymmetric unit (Z' = 2). The authors report a tetrahydrate with partially disordered water sites. In the present determination the water positions are also disordered, but the positions could be refined with a higher occupancy, raising the water stoichiometry to 4.25 water molecules per DTS unit. For the purposes of the present discussion, however, the name tetrahydrate will be retained. Full occupancy of all water positions would result in a

stoichiometry of 4.5 water molecules per DTS unit. Considering the relatively low stability of the hydrate in dry atmosphere, as observed by TG, it is possible that the crystal water is partially released depending on the handling of the sample prior to the diffraction experiment. It additionally points towards at least partial non-stoichiometric characteristics of this hydrate.

From the crystal structure, it is not obvious which water molecules are lost in the first dehydration step observed by TG. It is plausible that the non-coordinated water molecules O1W and O2W could leave more readily, especially since they are located in very small channels along (0 1 0) in the crystal structure, which allow a more facile egress than from the coordination sites of the sodium cations. This assumption is also based on the energetically weaker interaction of hydrogen bonds *vs*. ion coordination. On the other hand, approximately 2.4 moles of water leave the crystal lattice on the first dehydration step, thus the sodium coordination has to be broken for at least some of the water molecules. These sites are most likely the water molecules O4W and O5W, which bridge two sodium cations. Tonnessen *et al.*[23] report in their structure only half occupancy of one of these sites, while the present determination exhibits full occupancy for both water molecules, which is presumably due to rapid sample handling and hence less dehydration before the single-crystal diffraction experiment.

Due to the complex nature of this crystal structure and the presence of relatively heavy atoms, such as sodium and particularly iodine, not all hydrogen atom positions could be determined by X-ray crystallography. Thus, single-crystal neutron diffraction data was collected on the Laue diffractometer VIVALDI at the Institut Laue-Langevin (Grenoble, France). [35] These data enabled the accurate location of all hydrogen atom positions and their anisotropic refinement. As observed for DTA dihydrate, the bond lengths involving hydrogen atoms are longer in the neutron structure compared to the X-ray structure. In addition, all hydrogen atom positions could be deduced from the difference Fourier maps. Again, the terminal methyl groups show rather large ADPs for the hydrogen atoms consistent with rotational disorder. In addition, the hydrogen atoms on three of the water molecules (O1W, O2W and O4W) show large ADPs, which in the case of the former two can be explained by higher mobility of the water molecules in the crystal lattice, as they are not coordinated to sodium cations. O4W, however, is a bridging water molecule between two cations, thus its mobility should be reduced. The neutron beam time available permitted data collection for rotation around just one direction in the crystal. For a triclinic lattice in the Laue technique this will lead to a paucity of data along and near that axis which can result in exaggeration of the displacement parameters in that direction. For information about the hydrogen bond lengths, refer to the Supporting Information (Table S3).

Due to the coordination of both the host and the water molecules to the sodium cations, the DTS tetrahydrate exhibits a more complex crystalline network than DTA dihydrate. However, similar motifs of hydrogen bonding can be found in both crystal forms.The centrosymmetric dimer formation of the host molecule (protonated as well as deprotonated) through hydrogen bonds from the amide NH (N1 and N101) to the carboxylic acid group (O2 and O102) is realised in both forms. But whilst this motif links the DTA-water capsules in the dihydrate along the crystallographic *c*-axis (Figure 2), the dimers in the DTS tetrahydrate are separated by the water-coordinated sodium cations. The second motif is a water molecule (O3W) bridging between the two amide carbonyl groups of the same molecule (O103 and O104). This motif, however, is only realised for one of the two crystallographically independent host molecules in the DTS tetrahydrate. The amido carbonyl oxygen (O4) of the other molecule is involved in hydrogen bonding to three different water molecules: a bridging water molecule (O1W) between the amido carbonyl and sodium-coordinated oxygen atom of the carboxylate of the same molecule (Figure 7), a bridging water molecule (O6W) between the carbonyl oxygen and the carboxylate of an adjacent anion and a water molecule (O8Wb) bridging to another water molecule (O8Wa). This leaves one amido carbonyl group free for linking to the next DTS dimer through hydrogen bonding to the remaining free amido NH group (N2 and N102).

Even though the neutron single crystal experiment of DTS resulted in the determination of an accurate structural model, crystal lattice energy calculations using the PACHA algorithm were not feasible due to the high complexity of the coordination network.

The solvates

In addition to hydrated crystal forms, a series of DTA solvates were obtained by slow evaporation or slow cooling of solutions of DTA in a range of hydrogen-bond acceptor and donor solvents. The structures of three dimethylsulfoxide (DMSO) solvates, namely tetra-, di- and monosolvate, have been communicated previously and show an intriguing series of snapshots of the desolvation process during the crystal nucleation process.[26] This series of solvates demonstrates that of the three hydrogen-bond donor sites (carboxylic acid and two amide groups) the carboxylic acid is involved in the strongest hydrogen bonds and remains solvated as the DMSO bound to the other donors is removed.

Additional solvated crystal forms were obtained from N-dimethylformamide (DMF), tetrahydrofuran (THF), dioxane and methanol. Crystallographic data are listed in Table 1.

The DMF disolvate can be crystallised by evaporation of DMF solutions under ambient conditions, upon which large prisms form (Figure S5) that are relatively stable at room temperature. The single-crystal X-ray structure was determined in the orthorhombic space group *Pbca* with one molecular unit in the asymmetric unit ($Z' = 1$). The DTA molecule adopts an antiparallel conformation of the amide side-chains, similar to the DMSO tetra- and disolvates. Hydrogen bonding between the amide groups results in a brickwork-like network in the crystallographic *c*-plane, similar to that observed in the DMSO monosolvate. The solvent molecules are located in between two layers of this network. These show disorder over two positions for both molecules, with an occupancy of approximately 50:50 for one molecule and 30:70 for the other. The overall orientation of the envelope of the two solvent sites is, however, unchanged and the carbonyl oxygen atom remains almost unchanged in position. Consistent with the DMSO solvates, one DMF molecule interacts with the carboxylic acid group of the host molecule through hydrogen

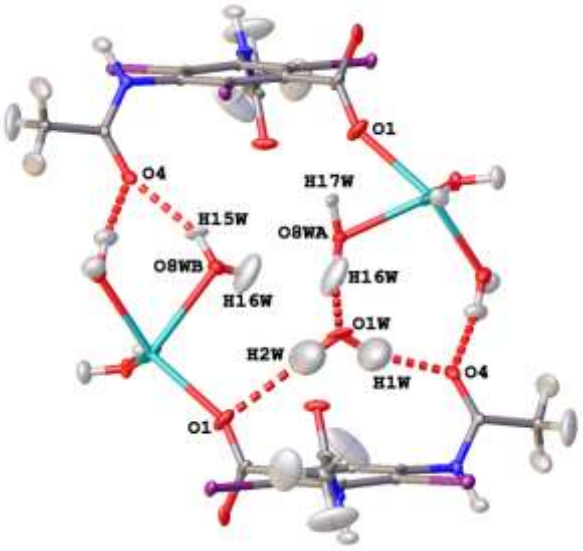

Figure 8. Section of the neutron single-crystal structure of the DTS tetrahydrate with disorder of the water molecule including O8W resolved. Atomic displacement ellipsoids are drawn at 30% probability.

Table 5. Geometric data of DTS tetrahydrate.

Interaction	D···A distance [Å]	D-H···A distance [Å]	D-H···A angle [°]
N1···O2	2.87(1)	1.85(2)[a]	172(1)
N101···O102	2.76(1)	1.70(2)[a]	174(1)
N2···O103	2.929(7)	1.93(1)[a]	165(1)
N102···O3	1.794(7)	1.76(1)[a]	174(1)
O1W···O1	3.48(3)	2.52(5)[a]	178(3)
O1W···O4	2.86(3)	1.92(5)[a]	164(3)
O2W···O101	2.81(2)	1.85(2)[a]	169(2)
O3W···O103	2.92(2)	1.97(3)[a]	174(2)
O3W···O104	3.14(1)	2.30(2)[a]	146(2)
O5W···O2	2.82(2)	1.88(2)[a]	169(3)
O5W···O7W	2.84(1)	1.88(2)[a]	169(2)
O6W···O4	2.86(1)	1.90(2)[a]	167(2)
O6W···O102	2.94(1)	2.01(2)[a]	173(1)
O7W···O2	2.88(2)	1.94(2)[a]	156(1)
O7W···O104	2.83(1)	1.89(2)[a]	164(2)
O8WA···O1W	2.75(2)	1.60(3)[a]	167(3)
O8WB···O4	2.96(3)	2.08(4)[a]	160(4)

[a] Hydrogen···acceptor distance derived from the neutron single-crystal data. Single atom descriptors (X) correspond to one DTA molecule, while 10X atom descriptors correspond to the second molecule.

bonding (Figure 8, Table 6). The second DMF molecule, on the other hand, interacts with the host molecule with an near linear O···I3 halogen bond and a somewhat more angular interaction to the iodine atom I2 (C-I···O angles of 173° and 167°, respectively, averaged over both solvent positions). These halogen bonds hold the DMF molecule in place in between the layers of DTA. Even though DMF and DMSO are related in size and shape, and although the DMF disolvate and the DMSO disolvate crystallise in the same space group, the overall packing of the two crystal structures is different. The DMSO disolvate shows only two interactions between the DTA molecules, one being a N-H···O hydrogen bond between two amide groups, the other the pseudo-centrosymmetric dimer formation via an I···O halogen bond involving the carboxylic acid group. All other hydrogen bonding groups interact with the incorporated solvent molecules. The DMF disolvate, on the other hand, consists of a brickwork-like layered structure of the DTA molecules (Figure 8a), in between which the solvent molecules are located (Figure 8b), which is comparable to that found in the DMSO monosolvate. This network of the host molecules is stabilised by N-H···O hydrogen bonds between the amide groups of adjacent molecules, and further stabilised by I···O halogen bonds involving the carboxylic acid group. The network shows the DTA molecules orienting in an AABB fashion, which is different to the ABAB orientation of the DMSO monosolvate.

Cooling a THF solution from room temperature to 4 °C results in the formation of a THF monosolvate. This molecular complex was characterised by X-ray crystallography in the monoclinic spacegroup $P2_1/n$ with one molecular unit in the asymmetric unit (Z' = 1). It is structurally related to the DMF disolvate and the DMSO monosolvate, even though the host molecule exhibits a *syn*-conformation of the amido substituents, unlike the *anti*-conformation found in the related solvates. The overall packing is brickwork-like similar to the DMF disolvate, but due to the *syn*-conformation of the host molecule, the orientation of the brickwork follows the ABAB motif found in the DMSO monosolvate (Figure S7). In fact, the THF monosolvate and the DMSO monosolvate are isostructural, even though the former crystallises in a lower symmetry space group.

The methanol monosolvate was obtained by cooling a supersaturated methanol solution of DTA to 4 °C. The crystal structure was determined in the triclinic space group $P\bar{1}$ with two molecular units in the asymmetric unit (Z' = 2). The overall packing resembles that of Form I of solvent-free DTA (*vide supra*). The DTA molecules form infinite chains connected through two different kinds of hydrogen bonds. The first mode connects two DTA molecules by two hydrogen bonds between an amido N-H and the carboxylic acid non-protonated oxygen atom into centrosymmetric dimers. These connect through hydrogen bonds of the free amido functionalities to the next dimer, forming a second centrosymmetric dimer, which connects the host molecules in an offset stack. The methanol guest is connected to these chains through hydrogen bonds from the protonated carboxylic acid oxygen atom to its hydroxyl oxygen atom, which furthermore hydrogen bonds to the oxygen atoms of the amido group of the next host. This links the individual chains of host molecules. Halogen bonds can be detected from I1, I3 and I103 to the carbonyl oxygen atoms of the amido groups of neighbouring DTA molecules. These interactions are an additional stabilising factor between the stacks of host molecules. Interestingly, this crystal form is the most unstable of all reported, as it readily transforms to the dihydrate, even when stored at low temperatures in the methanol mother liquor. When taken out of solution, the crystals crack and show strong pseudomorphosis due to loss of solvent at ambient conditions.

Finally, a mixed water/dioxane monosolvate (ratio of 1:1:1 water:dioxane:DTA) could be crystallised from dioxane solution at 4 °C. The X-ray crystal structure was determined by synchrotron radiation using beam line I19 at Diamond Lightsource, Oxfordshire, UK[36] in the monoclinic space group $P2_1/n$ with one molecular unit in the asymmetric unit (Z' = 1). The host

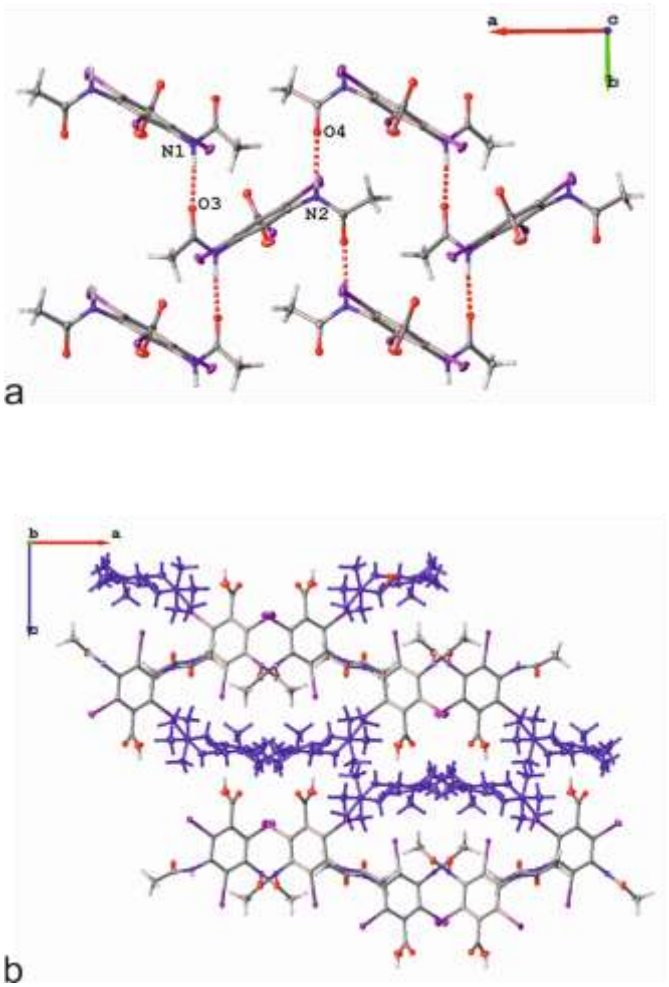

Figure 9. Brickwork-like crystal packing diagrams of the DMF disolvate: (a) individual hydrogen bonded layer viewed along the crystallographic *c*-axis and (b) location of the incorporated solvent (blue) in between the layers viewed along the crystallographic *b*-axis. Element colours: carbon (grey), nitrogen (blue), oxygen (red), iodine (purple), hydrogen (light grey). ADPs are drawn at 30% probability.

molecules adopt a *syn*-conformation. They assemble in centrosymmetric dimers, which are stabilised through two hydrogen bonds formed between the N-H of one amido group and the non-protonated oxygen atom of the carboxylic acid. The second amido group donates as well as accepts one hydrogen bond involving the incorporated water molecule, while the protonated oxygen atom of the acid moiety hydrogen bonds to the dioxane. In addition to these strong interactions, two halogen bonds are observed from I1 to an amido oxygen atom O4 and from I3 to the water molecule. This packing results in large cavities, which contain the solvent, and thus resembles the packing of the DTS tetrahydrate. Unlike the DTA tetartohydrate, the dioxane/water monosolvate does not incorporate water molecules purely as space fillers. The hydrogen atoms of the water molecules interact extensively with the host as well as the other solvent molecules, and are thus an inherent part of the structure.

Table 6 lists the interaction geometries and energies as calculated by PACHA. It is clear that the strongest interaction in all solvates involves the carboxylic acid group, followed by

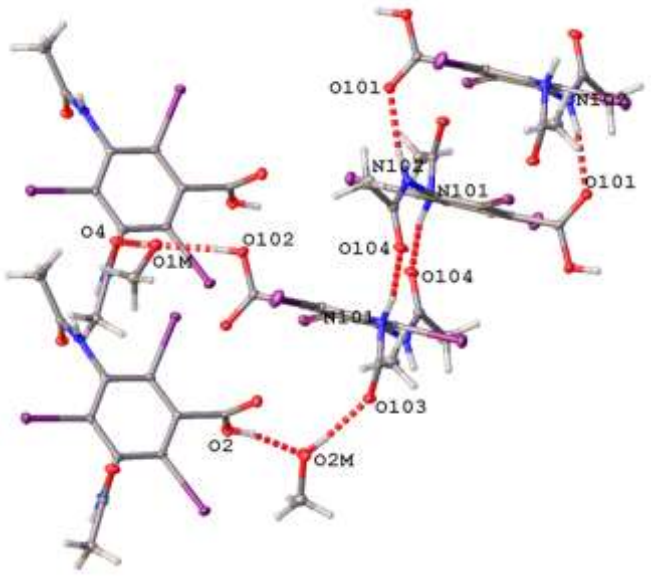

Figure 10. Representation of the hydrogen bonding observed in the DTA methanol monosolvate. Element colours: carbon (grey), nitrogen (blue), oxygen (red), iodine (purple), hydrogen (light grey). Atomic displacement ellipsoids are drawn at 30% probability.

homomeric interactions of the DTA through the amide moieties. In the case of the dioxane/water solvate, the second strongest interaction involves the incorporated water molecule, supporting the statement that the water is not only a space-filler in this solvate.

Structural relationships

Taking into account that DTA crystallises in three non-solvated and nine solvate forms, it is apparent that even though there are the same number of hydrogen bond donors and acceptors in the DTA molecule, the compound has a strong propensity to include solvent. This tendency could be due to the awkward shape of the molecule with an asymmetric tripodal arrangement of the substituents whilst having a generally flat core.[37] And even though three non-solvated crystal forms exist, it is possible that the solvent molecules stabilise intermittent crystal forms, i.e. the solvates, during the nucleation process of a crystallisation from solution.

Another interesting finding is that when DTA interacts purely with water, *i.e.* in the case of the dihydrate and the tetartohydrate, no halogen bonds are formed, in stark contrast to the non-aqueous solvates. Even though there are short contacts between oxygen and iodine atoms in the dihydrate, these are not shorter than the sum of the van der Waals radii, and PACHA calculations do not suggest that this is a stabilising interaction. This result indicates that the contact is a consequence of the final packing arrangement rather than being a driving force towards it. For the DTS tetrahydrate, no halogen bonds were observed, which is

likely due to the much stronger forces of the ionic interactions shaping the crystal packing.

As found for the DMSO solvate series, the solvent molecules in all of the solvates reported in the present work interact with the host molecules *via* the carboxylic acid group. The only exception is the tetarto hydrate, for which the water molecule fulfils a purely space-filling role without any interaction with the host. In addition, all solvents hydrogen bond to the host through an oxygen atom. This finding consolidates the hypothesis that the strongest hydrogen-bond donor will interact with the strongest hydrogen bond-acceptor.[38] It is very likely that during the nucleation process, this interaction is the last one to be broken in most hydrogen-bond acceptor solvents as observed in the case of the DMSO solvates.[26]

Table 6. Bond distances, geometries and energies of the solvated crystal structures of DTA.

Interaction	D···A distance [Å]	D-H···A angle [°]	Energy [kJ mol^{-1}]
DMF disolvate			
O1···O1SA	2.528(5)	169(2)	-53.1[a]
N1···O3	2.796(5)	159.9(2)	-34.5
N2···O4	2.807(6)	168.1(2)	-28.7
I1···O2	3.044(3)		-2.6
I2···O1SC	3.27(2)		-5.8[a]
I2···O1SD	2.97(1)		
I3···O1SC	2.92(2)		-7.7[a]
I3···O1SD	3.07(1)		
THF monosolvate			
O1···O1S	2.54(1)	167(6)	-36.6
N1···O4	2.80(1)	167(1)	-25.5
N2···O3	2.81(1)	173(1)	-27.8
I1···O2	3.184(8)		-5.9
I2···O2	3.063(6)		-2.7
Methanol monosolvate			
O2···O2M	2.509(4)	167(7)	-44.3
O102···O1M	2.567(3)	176(6)	-38.9
O1M···O4	2.678(4)	176(6)	-32.8
O2M···O103	2.718(5)	175(8)	-35.2
N1···O2	2.889(5)	171.0(3)	-32.6
N102···O102	2.842(4)	164.7(3)	-36.2[c]
N2···O3	2.866(5)	146.3(3)	-27.7
N101···O104	2.734(5)	165.1(3)	-33.0[c]
I1···O4	3.111(3)		[d]
I3···O103	3.032(3)		-5.9[c]
I103···O103	3.038(3)		[d]
Dioxane/water monosolvate			
O1···O2S	2.559(5)	168.4(5)	-52.2
N2···O2	2.841(5)	160.9(4)	-26.7
O3···O1W	2.744(5)	147(5)	-46.6
N1···O1W	2.844(5)	161.8(4)	-12.1
O1W···O1S	2.841(5)	165.6[b]	-21.8
I1···O4	2.986(3)		-5.3
I3···O1W	3.034(4)		-10.9[c]

[a] Averaged for two positions of disorder. [b] Angle after electrostatic optimisation of the water hydrogen atom positions. [c] Interaction energy is a sum of C-H···O hydrogen bond and halogen bond. [d] Interaction energy not to be deconvoluted from concomitant hydrogen bonds.

The conformation of the molecule does not follow any clear trend when compared across all of the crystal structures. In the case of the dihydrate, the DMSO disolvate and the THF monosolvate, the host adopts a *syn*-conformation, in which both carbonyl groups of the amide chains lie on one side of the rigid core. All other crystal structures show an *anti*-conformation.

Considering the crystal packing, the DTA DMSO monosolvate and the DTA THF monosolvate are isostructural, whilst the DTA brickwork-like network can also be found in the DTA DMF disolvate. The DTS tetrahydrate and the DTA dioxane water monosolvate show a close relationship in their packing, whilst the DTA tetartohydrate and the anhydrous Form I are isostructural. Even though these similarities do not follow a clear trend, *e.g.* the DTA DMF disolvate is closer related to the DMSO monosolvate than to the DMSO disolvate, this suggests that certain packing motifs, such as the brickwork-like hydrogen bonded layers, are stable enough to be realised in several crystal forms. Considering the importance of solvates in finding new polymorphs,[3a] as recently shown for furosemide,[39] for which the DMSO solvate desolvates to a different anhydrous crystal form than the solvates from THF, dioxane and DMF, understanding the interplay between host molecules and solvent guests, as well as the influence of the solvents on conformation and packing can hardly be overestimated.

Conclusion

In the present study we report and analyse nine crystal forms of diatrizoic acid (DTA) and one crystal form of its monosodium salt (DTS); eight of all crystal forms have been characterised by X-ray single-crystal diffraction. The structures of the dihydrate and tetrahydrated sodium salt have been additionally investigated by single-crystal neutron diffraction. All of the non-ionic structures have been examined by means of non-empirical lattice energy calculations (PACHA) in order to probe the interaction energies of the different intermolecular interactions.

The presence of nine solvated crystal forms (including three DMSO solvates previously reported) in addition to the three unsolvated modifications clearly shows that diatrizoic acid exhibits a strong tendency to include hydrogen-bond acceptor as well as donor solvents. However, this propensity cannot be attributed, as generally assumed, to an imbalance of hydrogen-bond donor and acceptor groups,[9b] as the molecule contains three of each.

It was found that the strongest interaction in all diatrizoic acid crystal forms involves the carboxylic acid moiety, which in most cases donates a hydrogen bond to the incorporated solvent. This strong interaction is likely to be retained during the gradual desolvation of pre-crystallisation clusters in solution, in which the interactions with lower energy are broken first to form new homomeric hydrogen bonds in the growing nucleus, while the strongest interaction is more likely to be retained.

While halogen bonding provides additional stabilisation for all of the solvates, the incorporation of water apparently switches off this interaction. This is likely due to more stable hydrogen bonding, such as the formation of a capsule in the dihydrate structure, in which a square of four water molecules are enclosed between two host molecules, which then pack into the final crystal structure in a way that is incompatible with halogen bonding interactions. Even though short contacts between the iodine residues and amide carbonyl groups are present, these do not contribute to the overall stabilising crystal lattice energy. Halogen bonds are observed, however, for the mixed dioxane / water ternary complex.

Diatrizoic acid represents a valuable case study in understanding the factors leading to the formation of solvate and non-solvated polymorphic crystal forms of pharmaceutical compounds. This study shows the clear preference of interaction between host and solute *via* strong hydrogen bond donor and acceptor groups, even when different hydrogen bonding sites are present. This is invaluable information to feed back into polymorph prediction algorithms, in order to optimise these and generate purely *in silico* polymorph and solvent screening tools.[40]

Acknowledgements

We would like to thank the Institute Laue-Langevin, Grenoble, France, and the ANSTO, Lucas Heights, Australia, for the allocation of neutron beam time (proposal numbers 5-12-250 and P1289, respectively). In addition, we are grateful for the opportunity to measure the crystal structure of the DTA tetartohydrate and the DTA dioxane/water monosolvate on the beamline I19 at Diamond Light Source, Didcot, United Kingdom, with beam time allocated to the regional team of Newcastle and Durham Universities. We thank the Engineering and Physical Sciences Research Council for funding grant number EP/F063229/1.

Keywords: polymorphism • crystallography • neutron diffraction • halogen bonds • lattice energy calculation

[1] J. Bernstein, *Polymorphism in Molecular Crystals*, Clarendon Press, Oxford, **2002**.

[2] D. J. W. Grant, in *Polymorphism in Pharmaceutical Solids, Vol. 95* (Ed.: H. G. Brittain), Marcel Dekker Inc., New York, **1999**, pp. 1-33.

[3] a) U. J. Griesser, in *Polymorphism* (Ed.: R. Hilfiker), Wiley-VCH, Weinheim, Germany, **2006**, pp. 211-233; b) K. R. Morris, in *Polymorphism in Pharmaceutical Solids, Vol. 95* (Ed.: H. G. Brittain), Marcel Dekker Ltd, New York, **1999**, pp. 125-181.

[4] J. W. Steed, *Trends Pharmacol. Sci.* **2013**, *34*, 185-193.

[5] a) J. Bernstein, *Cryst. Growth Des.* **2011**, *11*, 632-650; b) C.-H. Gu, V. Young, D. J. W. Grant, *J. Pharm. Sci.* **2001**, *90*, 1878-1890; c) S. Byrn, R. Pfeiffer, M. Ganey, C. Hoiberg, G. Poochikian, *Pharm. Res.* **1995**, *12*, 945-954; d) L.-F. Huang, W.-Q. Tong, *Adv. Drug Delivery Rev.* **2004**, *56*, 321-334.

[6] See ICH guideline Q6A Point 3.3.1

[7] a) S. L. Morissette, S. Soukasene, D. Levinson, M. J. Cima, O. Almarsson, *Proc. Natl. Acad. Sci. U. S. A.* **2003**, *100*, 2180-2184; b) J. Bauer, S. Spanton, R. Henry, J. Quick, W. Dziki, W. Porter, J. Morris, *Pharm. Res.* **2001**, *18*, 859-866.

[8] a) A. Caridi, S. A. Kulkarni, G. Di Profio, E. Curcio, J. H. ter Horst, *Cryst. Growth Des.* **2014**, *14*, 1135-1141; b) R. J. Davey, S. L. M. Schroeder, J. H. ter Horst, *Angew. Chem. Int. Ed.* **2013**, *52*, 2166-2179.

[9] a) L. Infantes, L. Fabian, W. D. S. Motherwell, *CrystEngComm* **2007**, *9*, 65-71; b) C. H. Gorbitz, H.-P. Hersleth, *Acta Crystallogr. B* **2000**, *B56*, 526-534.

[10] C. A. Hunter, J. F. McCabe, A. Spitaleri, *CrystEngComm* **2012**, *14*, 7115-7117.

[11] a) G. R. Desiraju, *J. Chem. Sci.* **2010**, *122*, 667-675; b) A. Gavezzotti, *Molecular Aggregation: Structure Analysis and Molecular Simulation of Crystals and Liquids*, Oxford University Press, New York, USA, **2007**; c) E. Corradi, S. V. Meille, M. T. Messina, P. Metrangolo, G. Resnati, *Angew. Chem.* **2000**, *112*, 1852-1856.

[12] a) J. Bernstein, R. E. Davis, L. Shimoni, N.-L. Chang, *Angew. Chem. Int. Ed.* **1995**, *34*, 1555-1573; b) G. A. Jeffrey, *An Introduction to Hydrogen Bonding*, 1st ed., Oxford Univeristy Press, Oxford, **1997**; c) S. Schultes, C. de Graaf, H. Berger, M. Mayer, A. Steffen, E. E. J. Haaksma, I. J. P. de Esch, R. Leurs, O. Kramer, *MedChemComm* **2012**, *3*, 584-591.

[13] a) K. Fucke, J. W. Steed, *Water* **2010**, *2*, 333-350; b) C. C. Wilson, *Z. Kristallogr.* **2005**, *220*, 385-398.

[14] S. Grabowsky, D. Jayatilaka, R. F. Fink, T. Schirmeister, B. Engels, *Z. Anorg. Allg. Chem.* **2013**, *639*, 1905-1921.

[15] a) K. Fucke, G. J. McIntyre, C. Wilkinson, M. Henry, J. A. K. Howard, J. W. Steed, *Cryst. Growth Des.* **2012**, *12*, 1395-1401; b) K. Fucke, K. M. Anderson, M. H. Filby, M. Henry, J. Wright, S. A. Mason, M. J. Gutmann, L. J. Barbour, C. Oliver, A. W. Coleman, J. L. Atwood, J. A. K. Howard, J. W. Steed, *Chem. Eur. J.* **2011**, *17*, 10259-10271; c) M. Henry, *ChemPhysChem* **2002**, *3*, 561-569.

[16] a) C. B. Aakeroy, M. Baldrighi, J. Desper, P. Metrangolo, G. Resnati, *Chem. Eur. J.* **2013**, *19*, 16240-16247; b) M. Baldrighi, G. Cavallo, M. R. Chierotti, R. Gobetto, P. Metrangolo, T. Pilati, G. Resnati, G. Terraneo, *Mol. Pharm.* **2013**, *10*, 1760-1772.

[17] a) L. Meazza, J. A. Foster, K. Fucke, P. Metrangolo, G. Resnati, J. W. Steed, *Nat. Chem.* **2013**, *5*, 42-47; b) A. Priimagi, G. Cavallo, P. Metrangolo, G. Resnati, *Acc. Chem. Res.* **2013**, *46*, 2686-2695; c) D. Yan, D.-K. Bučar, A. Delori, B. Patel, G. O. Lloyd, W. Jones, X. Duan, *Chem. Eur. J.* **2013**, *19*, 8213-8219.

[18] C. B. Aakeröy, S. Panikkattu, P. D. Chopade, J. Desper, *CrystEngComm* **2013**, *15*, 3125-3136.

[19] M. Cametti, K. Raatikainen, P. Metrangolo, T. Pilati, G. Terraneo, G. Resnati, *Org. Biomol. Chem.* **2012**, *10*, 1329-1333.

[20] *Pharmacopoeia Europaea 8.1*, Deutscher Apotheker Verlag, Stuttgart & Govi-Verlag GmbH, Eschborn, **2014**.

[21] *United States Pharmacopoeia Vol 37*, The Stationary Office, Norwich, England, **2014**.

[22] R. K. Khankari, D. J. W. Grant, *Thermochim. Acta* **1995**, *248*, 61-79.

[23] L. E. Tonnessen, B. F. Pedersen, J. Klaveness, *Acta Chem. Scand.* **1996**, *50*, 603-608.

[24] C. Peng, K. G. Li, X. Y. Cao, T. T. Xiao, W. X. Hon, L. F. Zheng, R. Guo, M. W. Shen, G. X. Zhang, X. Y. Shi, *Nanoscale* **2012**, *4*, 6768-6778.

[25] V. A. Folen, G. Schwartzman, M. Maienthal, W. L. Brannon, *J. Assoc. Off. Anal. Chem.* **1978**, *61*, 72-75.

[26] K. Fucke, J. A. K. Howard, J. W. Steed, *Chem. Commun.* **2012**, *48*, 12065-12067.

[27] K. Fucke, M. J. G. Peach, J. A. K. Howard, J. W. Steed, *Chem. Commun.* **2012**, *48*, 9822-9824.

[28] a) D. R. Turner, M. Henry, C. Wilkinson, G. J. McIntyre, S. A. Mason, A. E. Goeta, J. W. Steed, *J. Am. Chem. Soc.* **2005**, *127*, 11063-11074; b) D. R. Turner, M. B. Hursthouse, M. E. Light, J. W. Steed, *Chem. Commun.* **2004**, 1354-1355.

[29] O. V. Dolomanov, L. J. Bourhis, R. J. Gildea, J. A. K. Howard, H. Puschmann, *J. Appl. Crystallogr.* **2009**, *42*, 339-341.

[30] a) A. O. F. Jones, M. H. Lemee-Cailleau, D. M. S. Martins, G. J. McIntyre, I. D. H. Oswald, C. R. Pulham, C. K. Spanswick, L. H. Thomas, C. C. Wilson, *Phys. Chem. Chem. Phys.* **2012**, *14*, 13273-13283; b) C. C. Wilson, N. Shankland, A. J. Florence, *J. Chem. Soc. Faraday Trans.* **1996**, *92*, 5051-5057.

[31] Z. Skoko, S. Zamir, P. Naumov, J. Bernstein, *J. Am. Chem. Soc.* **2010**, *132*, 14191-14202.
[32] A. Burger, R. Ramberger, *Mikrochim. Acta* **1979**, *2*, 259-271.
[33] A. Burger, R. Ramberger, *Mikrochim. Acta* **1979**, *2*, 273-316.
[34] S. N. Ivashevskaya, J. van de Streek, J. E. Djanhan, J. Bruening, E. Alig, M. Bolte, M. U. Schmidt, P. Blaschka, H. W. Hoeffken, P. Erk, *Acta Crystallogr. B* **2009**, *B65*, 212-222.
[35] a) C. Wilkinson, J. A. Cowan, D. A. A. Myles, F. Cipriani, G. J. McIntyre, *Neutron News* **2002**, *13*, 37-41; b) G. J. McIntyre, M. H. Lemee-Cailleau, C. Wilkinson, *Physica B* **2006**, *385-86*, 1055-1058.
[36] H. Nowell, S. A. Barnett, K. E. Christensen, S. J. Teat, D. R. Allan, *J. Synchrotron Rad.* **2012**, *19*, 435-441.
[37] K. M. Anderson, M. R. Probert, A. E. Goeta, J. W. Steed, *CrystEngComm* **2011**, *13*, 83-87.
[38] a) C. B. Aakeröy, N. Schultheiss, J. Desper, *J. Mol. Struct.* **2010**, *972*, 35-40; b) M. C. Etter, *Acc. Chem. Res.* **1990**, *23*, 120-126.
[39] V. S. Minkov, A. A. Beloborodova, V. A. Drebushchak, E. V. Boldyreva, *Cryst. Growth Des.* **2013**, *14*, 513-522.
[40] a) S. L. Price, *Chem. Soc. Rev.* **2014**, *43*, 2098-2111; b) S. Mohamed, D. A. Tocher, S. L. Price, *Int. J. Pharm.* **2011**, *418*, 187-198; c) D. E. Braun, P. G. Karamertzanis, S. L. Price, *Chem. Commun.* **2011**, *47*, 5443-5445; d) S. L. Price, *Acc. Chem. Res.* **2009**, *42*, 117-126; e) J. Kendrick, G. A. Stephenson, M. A. Neumann, F. J. J. Leusen, *Cryst. Growth Des.* **2013**, *13*, 581-589; f) M. A. Neumann, F. J. J. Leusen, J. Kendrick, *Angew. Chem. Int. Ed.* **2008**, *47*, 2427-2430; g) M. D. Eddleston, K. E. Hejczyk, E. G. Bithell, G. M. Day, W. Jones, *Chem. Eur. J.* **2013**, *19*, 7874-7882.

Received: ((will be filled in by the editorial staff))
Revised: ((will be filled in by the editorial staff))
Published online: ((will be filled in by the editorial staff))

DOI: 10.1002/chem.201xxxxxx

Entry for the Table of Contents
Layout 2:

FULL PAPER

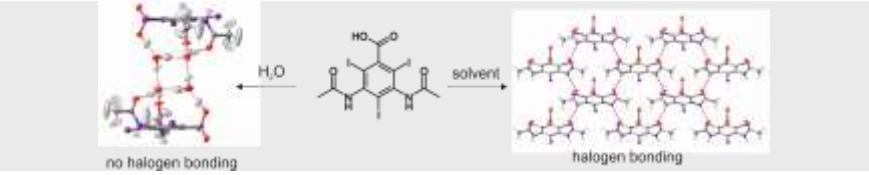

Switch it off: Diatrizoic acid crystallises in two hydrated, three non-solvated and nine solvated crystal forms. The ultra-stable hydrogen-bonded dihydrate capsule does not allow for halogen bonding, whilst all solvated forms show this interaction. Several crystal packing motifs reveal overall similar supramolecular interactions. The strongest solvent-host interaction involves the carboxylic acid, likely last broken in the nucleation process.

Pharmaceuticals

Katharina Fucke, Garry J. McIntyre, Clive Wilkinson, Alison J. Edwards, Judith A. K. Howard, Jonathan W. Steed**

■■ – ■■

Insights into the Crystallisation Process from Anhydrous, Hydrated and Solvated Crystal Forms of Diatrizoic Acid